

Safe Networked Robotics with Probabilistic Verification

Sai Shankar Narasimhan^{1,*,\dagger}, Sharachchandra Bhat^{1,*}, and Sandeep P. Chinchali¹

Abstract—Autonomous robots must utilize rich sensory data to make safe control decisions. To process this data, compute-constrained robots often require assistance from remote computation, or the cloud, that runs compute-intensive deep neural network perception or control models. However, this assistance comes at the cost of a time delay due to network latency, resulting in past observations being used in the cloud to compute the control commands for the present robot state. Such communication delays could potentially lead to the violation of essential safety properties, such as collision avoidance. This paper develops methods to ensure the safety of robots operated over communication networks with *stochastic* latency. To do so, we use tools from formal verification to construct a shield, i.e., a run-time monitor, that provides a list of safe actions for any delayed sensory observation, given the expected and maximum network latency. Our shield is minimally intrusive and enables networked robots to satisfy key safety constraints, expressed as temporal logic specifications, with desired probability. We demonstrate our approach on a real F1/10th autonomous vehicle that navigates in indoor environments and transmits rich LiDAR sensory data over congested WiFi links.

Index Terms—Formal Methods, Networked Robotics, Teleoperation, Probabilistic Verification

I. INTRODUCTION

Today, an increasing number of robotic applications require remote assistance, ranging from remote manipulation for surgery [1] to emergency take-over of autonomous vehicles [2]. Teleoperation is often used to collect rich demonstration data for imitation learning [3] or even to control fleets of food delivery robots from command centers hundreds of miles away [4]. For robots operated over communication networks, network latency is a key concern for safe operation since actuation based on delayed state information can lead to unsafe behavior.

Despite the rise of robots operating over communication networks, we lack formal guarantees for their safe operation. Today’s approaches for robotic safety range from reachability analysis [5], [6], [7], [8] to shielding that restricts unsafe actions based on a formal safety specification [9], [10], [11], [12]. However, there is little to no research that provides such rigorous safety analysis for networked robotics. This paper asks: *How do we ensure safe networked control over wireless networks with stochastic communication delays?*

Communication delay is the cumulative time delay in sending the observation to the cloud and receiving an action back at the robot. We develop the intuition that if the interaction between a remotely controlled robot and the surrounding

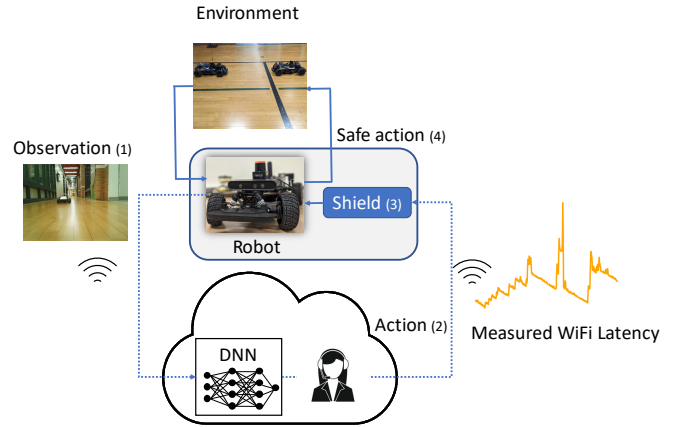


Fig. 1: **Safe Networked Control for Robotics:** A resource-constrained robot transfers sensor observations (RGB-D images or LiDAR point clouds) through a wireless network with stochastic latency. At the receiving end, a control module or a human teleoperator processes the observation to generate the corresponding action. The action is filtered by the shield, which enforces a particular safety specification that the robot has to maintain. The filtered, “safe” action is then executed by the robot.

environment can be modeled as a Markov Decision Process (MDP) (which is often the case), then the communication delay is analogous to sensing or actuation delays. A plethora of work has modeled MDPs with sensing and actuation delays for Networked Control Systems (NCS) [13], [14], [15]. However, these studies often rely on assumptions such as constant delays [13], [15] or that the delay between consecutive time steps cannot reduce [14]. In this paper, we propose *Delayed Communication* MDP, a novel approach to model MDPs with delays that aligns naturally with the transmission of observations and control commands when operating a robot via wireless networks in practice.

Fig. 1 shows our approach, tested on a real F1/10th autonomous racecar [16] controlled over a wireless link. Our approach is extremely general – we can either have a remote human teleoperator or an automatic controller running in the cloud. For example, if our robot is constrained by computing, memory, or power, it can offload the inference of a Deep Neural Network (DNN) perception model and deep reinforcement learning (RL) controller to the cloud. First, sensor observations (RGB-D images or LiDAR point clouds) are transferred via wireless links (step 1) and processed to compute the corresponding control command (step 2). The control command is transmitted back to the robot and filtered by the shield. The shield is a run-time monitor, constructed offline, that disallows actions that violate a formal safety specification. Since the shield runs on the robot, it has access to the delay corresponding to the received control command.

*Equal contribution. [†]Corresponding author.

¹Sai Shankar Narasimhan, Sharachchandra Bhat, and Sandeep P. Chinchali are affiliated with the department of Electrical and Computer Engineering, The University of Texas at Austin, USA. {nsaishankar, sharachchandra, sandeepc}@utexas.edu

Finally, the robot implements the shielded action (steps 3-4), which guarantees safe behavior amidst stochastic network latency. We design the shield using tools from formal verification [17], given knowledge of the network latency and a model of the surrounding environment’s behavior.

Shields, as implemented in [9], provide an absolute measure of safety. For networked control with stochastic network latency, patching the cloud control commands with shields results in perfectly safe operation at the cost of task efficiency. In this paper, we propose a shield synthesis approach that, when combined with the cloud controller, allows the networked control system to meet safety requirements with a desired probability. Our experimental findings indicate that a slight reduction in the desired safety probability leads to a significant increase in task efficiency. In this paper,

- 1) We present the *Delayed Communication* MDP, a novel approach that accurately models the interaction between a remotely controlled robot and the environment, in the presence of stochastic network latency.
- 2) We propose an algorithm to synthesize a shield that, when executed with the cloud controller, guarantees the desired probability of satisfying a safety property.
- 3) We demonstrate our approach in simulation as well as on an F1/10th autonomous vehicle that must closely (and safely) follow an unpredictable leader in indoor environments over congested wireless networks (Fig. 2).

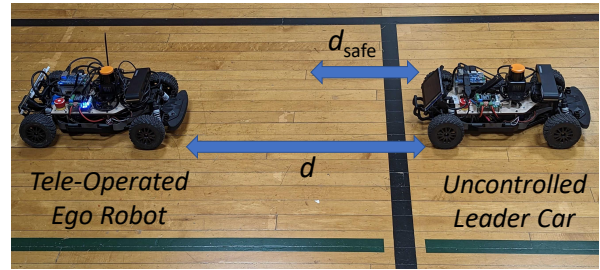
II. RELATED WORK

We now survey how our work relates to cloud robotics, networked control systems, shielding and formal methods.

Cloud Robotics: Cloud robotics [18], [19] studies how resource-constrained robots can offload real-time inference [20], [21], mapping and control to powerful remote servers [22]. Recent work ([23]) mitigates network latency using motion segmentation and motion synthesis by predicting the intent of the teleoperator, and synthesizing it locally on the robot (shared autonomy). This approach does not scale well for dealing with safety of resource-constrained robots, which we address in this work.

Delayed MDPs: Numerous prior works have addressed sensing and actuation delays in MDPs [13], [14], [15], [24], by making restrictive assumptions about the delay transitions. For example, the delay is constant in [13] and [15], while the delay can only increase or remain constant between consecutive time steps in [14], leading to a halt in decision-making when the delay reaches the assumed maximum limit. In contrast, we make no such assumptions. Additionally, prior works have focused on the delay in feedback [24] or cost collection ([14], [15]) in the RL setting. However, our objective is to *formally verify the safety of networked control systems* with stochastic communication delays.

Shielding and Safe Reinforcement Learning: Our work builds upon techniques developed for safe RL. In particular, the shielding approach [9], [12] involves synthesizing a minimally intrusive run-time monitor that overwrites the agent’s action only if it leads to a violation of the desired safety specification, aiding in safe exploration [10]. Recent work



$$\Pr(s \models \Box \neg S_{\text{unsafe}}) \geq \delta ; S_{\text{unsafe}} = \{d : d < d_{\text{safe}}\}$$

Fig. 2: **Hardware Setup:** Our ego robot (back) must follow a leader car with an unknown acceleration profile. The task is to get as close as possible to the leader while always maintaining a safe distance of more than d_{safe} (as shown in the LTL specification above) in the presence of network delay.

relaxes assumptions on the knowledge of the environment and makes the shielding approach more practically applicable [25], [26]. Since safety is an absolute notion, enforcing safety may restrict exploration and lead to sub-optimal policies. To provide flexibility, probabilistic shields are defined in [11], which trade off safety for better exploration while learning. Building on this, recent work implements probabilistic shields through probabilistic logic programs [27]. The definition of the probabilistic shield in [28] is similar to ours but only provides empirical estimates for safety probability. In contrast, our approach ensures that the desired probabilistic safety guarantee is achieved. Another probabilistic shielding approach [29] focuses specifically on synthesizing shields that satisfy *bounded* temporal logic specifications. While the above-mentioned works deal with shielding for safe RL, we formulate a novel shielding approach for networked control systems and validate it on a real robot.

Continuous State Spaces: The previous approaches mostly deal with finite state models usually obtained from an abstraction of the original continuous state-space dynamical system. On the other hand, Hamilton-Jacobi reachability analysis [5], [6] and Control Barrier Function methods [7], [8], [30] formulate the safe control problem for the continuous system. However, these methods cannot express rich safety properties, such as “always keep a minimum distance between two vehicles when the network latency is above a threshold and visit the landmark before reaching the goal”, which is possible using our approach.

III. BACKGROUND

A probability distribution over a finite set X is a function $p : X \rightarrow [0, 1]$ with $\sum_{x \in X} p(x) = 1$. A *Markov Decision Process* (MDP) is a tuple $\langle S, \text{Init}, \text{Act}, \mathbb{A}, \mathbb{P} \rangle$, where S is a finite state set, Init is a probability distribution over S and Act is a finite set of actions. The transition probability function $\mathbb{P} : S \times \text{Act} \times S \rightarrow [0, 1]$ is a conditional probability distribution and hence satisfies $\sum_{s' \in S} \mathbb{P}(s' | s, a) = 1$ for every state-action pair $(s, a) \in S \times \mathbb{A}(s)$, where $\mathbb{A}(s) = \{a \in \text{Act} \mid \exists s' \in S \text{ s.t. } \mathbb{P}(s' | s, a) \neq 0\}$ is the set of available actions for the state s . A policy π is defined as a mapping from states to actions, $\pi : S \rightarrow \text{Act}$.

We will now introduce safety properties and our approach using the hardware setup in Fig. 2, where a resource-

constrained mobile robot must safely follow an unpredictable leader while being controlled remotely over a wireless link with stochastic network delays. Henceforth, we will use the term *agent* to indicate any controlled entity like the robot and *environment* for uncontrolled entities (like the leader car). The agent and the environment together form the *system*.

We now introduce a formalism to capture our desired notion of safety for the system. We first define S_{unsafe} to be the set of all *unsafe states*. For example, in our hardware setup, an unsafe state is one where the distance between the two cars, d , is less than the safety threshold d_{safe} as shown in Fig. 2. Then, we define the system to be safe if it never reaches any state in S_{unsafe} . This can be encapsulated by the Linear Temporal Logic (LTL) [17] safety specification $\Box \neg S_{\text{unsafe}}$, which translates to “always (\Box) never (\neg) be in an unsafe state”. This formalism is useful since our notion of safety is now equivalent to determining the probability with which the system *satisfies the safety specification* $\varphi = \Box \neg S_{\text{unsafe}}$, which can be done efficiently. We use $V_{\mathcal{M},\varphi}^{\pi}(s)$ to represent the probability of satisfying φ , while executing the policy π starting from the state $s \in S$. The probability with which the system satisfies φ is then given by the safety probability of the initial states, $\mathbb{E}_{s \sim \text{Init}} [V_{\mathcal{M},\varphi}^{\pi}(s)]$.

We now briefly describe how to compute the safety probabilities $V_{\mathcal{M},\varphi}^{\pi}$. First, note that the safety property $\varphi = \Box \neg S_{\text{unsafe}}$ can be cast into a reachability property $\psi = \diamond S_{\text{unsafe}}$, which refers to “eventually (\diamond) reach any unsafe state”. Now, the probability of satisfying this reachability property or the reachability probability $V_{\mathcal{M},\psi}^{\pi}(s)$ is the unique solution to the following system of equations [17]:

$$\begin{aligned} \text{if } s \in S_{\text{unsafe}} \Rightarrow V_{\mathcal{M},\psi}^{\pi}(s) = 1; \text{ if } s \notin S_{\text{unsafe}} \Rightarrow V_{\mathcal{M},\psi}^{\pi}(s) = 0, \\ \text{else } V_{\mathcal{M},\psi}^{\pi}(s) = \mathbb{E}_{s' \sim \mathbb{P}(s'|s,\pi(s))} [V_{\mathcal{M},\psi}^{\pi}(s')]. \end{aligned} \quad (1)$$

This can be solved using value iteration. Then, the safety probabilities can be computed using the relation $V_{\mathcal{M},\varphi}^{\pi}(s) = 1 - V_{\mathcal{M},\psi}^{\pi}(s) \forall s \in S$. We denote the minimum and maximum probabilities of satisfying the safety property φ , across any policy, as $V_{\mathcal{M},\varphi}^{\min}(s)$ and $V_{\mathcal{M},\varphi}^{\max}(s)$ respectively. These quantities are independent of the policy and describe the range of safety probabilities that the system can attain. We refer the readers to [17] for details on how they can be computed. We also denote the minimum and maximum safety probability of the property φ for a *state-action pair* $(s, a) \in S \times \mathbb{A}(s)$ by $Q_{\mathcal{M},\varphi}^{\min}(s, a)$ and $Q_{\mathcal{M},\varphi}^{\max}(s, a)$ respectively. For example, $Q_{\mathcal{M},\varphi}^{\max}(s, a)$ is computed as

$$Q_{\mathcal{M},\varphi}^{\max}(s, a) = \mathbb{E}_{s' \sim \mathbb{P}(s'|s,a)} [V_{\mathcal{M},\varphi}^{\max}(s')]. \quad (2)$$

We denote the policy corresponding to the maximum safety probability, $V_{\mathcal{M},\varphi}^{\max}(s)$, as the optimally safe policy $\pi_{\mathcal{M},\varphi}^{\text{safe}}$, defined as $\pi_{\mathcal{M},\varphi}^{\text{safe}}(s) = \text{argmax}_a Q_{\mathcal{M},\varphi}^{\max}(s, a)$. These quantities are necessary to define our *shield* that can ensure a desired safety probability δ for the networked controlled system. For an MDP $\mathcal{M} = \langle S, \text{Init}, \text{Act}, \mathbb{A}, \mathbb{P} \rangle$, a shield ([9], [11]) is a function, $C : S \rightarrow 2^{\text{Act}}$, that maps every state $s \in S$ to a subset of $\mathbb{A}(s)$. During runtime, the shield overwrites the policy only if $\pi(s) \notin C(s)$.

IV. PROBLEM FORMULATION

In this section, we will explain our problem setting and formally define our safe networked control problem. We make the following three key assumptions in this work:

- The agent-environment interaction is available as an MDP $\mathcal{M}_b = \langle S, \text{Init}, \text{Act}, \mathbb{A}, \mathbb{P} \rangle$, where the state and action sets are discrete and finite. For the continuous case, we obtain finite sets by abstracting the continuous state and action spaces. We term this as the *Basic* MDP. In our hardware setup, the state set S consists of bins of possible distances between the cars, the action set Act consists of bins of allowed ego-robot velocities and the transition probability function \mathbb{P} captures the leader’s unpredictability modeled using an assumed range of velocities. This is a standard assumption since the offline computation of safe control policies typically requires knowledge of the agent-environment interaction [5], [11], [28].
- We assume a sufficient understanding of the stochasticity in communication delay, which we model as a transition probability function \mathbb{P}_{τ} with an upper bound τ_{max} on the delay. Later, in Sec. VI, we show how to obtain \mathbb{P}_{τ} from the collected time-series datasets of communication delays. Additionally, wireless systems have a maximum latency, such as a dedicated “slice” of a 5G network for ultra-low latency communication. Therefore, τ_{max} can be easily set by a wireless standard [31].
- Finally, we assume the cloud controller π_{cloud} is available as a mapping from the state set S to the action set Act for the *Basic* MDP. For the discrete case, this mapping is trivial as it is π_{cloud} itself. For the continuous case, the mapping can be easily obtained even for complex DNN controllers [32]. Later, we show how to relax this assumption for cases like human-teleoperation. Note that the cloud controller π_{cloud} is unaware of the communication delay.

We now explain the practical effects of stochastic communication delay on networked control systems. Consider an agent sending timestamped observations to the cloud. The cloud processes these observations to extract the system state information, generates a corresponding action, and appends the same timestamp to it before sending it back to the agent. We define communication delay as the time difference between the current time and the timestamp of the received action. Formally, at time t , the communication delay is τ_t if the received action, a_t , corresponds to the delayed state $s_{t-\tau_t}$. We refer to $s_{t-\tau_t}$ as the latest available system state at time t . Between two consecutive time steps t and $t+1$, only one of the following three events can occur.

- *Case 1:* The agent receives no action from the cloud. This implies that the latest available system state at $t+1$ is still $s_{t-\tau_t}$ and the delay $\tau_{t+1} = \tau_t + 1$.
- *Case 2:* The agent receives an action with a timestamp equal to the current time, implying no delay, i.e., $\tau_{t+1} = 0$.
- *Case 3:* The agent receives an action with an older timestamp, implying $\tau_{t+1} > 0$ and $\tau_{t+1} \leq \tau_t$.

To model these events, we represent the delay transitions as a conditional probability distribution $\mathbb{P}_{\tau}(\tau_{t+1} | \tau_t)$, $\mathbb{P}_{\tau} :$

$\Omega \times \Omega \rightarrow [0, 1]$ where $\Omega = \{0, 1, \dots, \tau_{\max}\}$ is the set of integer delay values. As the delay cannot increase by more than 1 (*Case 1*), we have $\mathbb{P}_\tau(\tau_{t+1} | \tau_t) = 0$ if $\tau_{t+1} > \tau_t + 1$.

Problem: We are given the *Basic* MDP, \mathcal{M}_b , that models the agent-environment interaction, the delay transition probability function \mathbb{P}_τ with an upper bound on delay τ_{\max} , and the cloud controller π_{cloud} . Our objective is to design a shield that minimally modifies the actions received by the agent from the cloud during runtime, such that the system satisfies safety specification $\square \neg S_{\text{unsafe}}$ with probability δ , where S_{unsafe} is the set of unsafe states.

V. APPROACH

The *Basic* MDP \mathcal{M}_b does not account for the presence of stochastic communication delay. Therefore, from \mathcal{M}_b we first create a *Delayed Communication* MDP (DC-MDP) that accounts for the delay and use this to construct the shield that ensures safe networked control. To do so, note that in the presence of delay, the state transition model can no longer rely only on s_t and a_t to determine the next state s_{t+1} . This is because s_t is not known when the delay is not zero. Note that when the delay at time t is τ_t , the maximum information available about the system is the latest observed system state $s_{t-\tau_t}$ and the sequence of actions executed from $t-\tau_t$ to $t-1$, $a_{t-\tau_t}, \dots, a_{t-1}$. Therefore, determining whether an action a_t is safe with respect to the property $\square \neg S_{\text{unsafe}}$ should intuitively rely on $s_{t-\tau_t}$ and $a_{t-\tau_t}, \dots, a_{t-1}$.

A. Delayed Communication Markov Decision Processes

We incorporate the maximum information available at any time step in the presence of delay into the state of the DC-MDP. As explained earlier, if the delay at t is τ_t , then we only have access to the recently observed system state, $s_{t-\tau_t}$ and the series of actions executed from $t-\tau_t$ to $t-1$, $(a_{t-\tau_t}, \dots, a_{t-1})$, which we call the action buffer. Note that the action buffer's length is the delay τ_t , which can vary. So, we introduce $\tau_{\max} - \tau_t$ number of placeholder actions, ϕ , to ensure the action buffer's length is always τ_{\max} . Now, we define the state at time t , x_t , as $(s_{t-\tau_t}, (a_{t-\tau_t}, \dots, a_{t-1}, \phi, \dots, \phi), \tau_t)$ and the state space for the DC-MDP as $X_d \in S \times (\text{Act} \cup \{\phi\})^{\tau_{\max}} \times \Omega$, where $\Omega = \{0, 1, \dots, \tau_{\max}\}$ is the set of all possible delays. This expanded state space increases exponentially with τ_{\max} . However, with delays of 4 or 5 time steps, seen in practice, the computation is tractable. Without loss of generality, the initial delay, τ_0 is 0, i.e., the latest available system state at the beginning of any task execution is the initial system state. Let s_{Init} be the set of initial states for \mathcal{M}_b , then we define the initial state probability distribution of the DC-MDP, Init_d , to only have non-zero probabilities for the states in the list $s_{\text{Init}} \times \{(\phi, \phi, \dots, \phi)\} \times \{0\}$.

Consider the state $x_t = (s_{t-\tau_t}, (a_{t-\tau_t}, \dots, a_{t-1}), \tau_t)$ and the action a_t . We now relate the three possible events described in Sec. IV to the state transitions in X_d .

- *Case 1:* $\tau_{t+1} = \tau_t + 1$. The latest available system state remains the same. Thus x_{t+1} is $(s_{t-\tau_t}, (a_{t-\tau_t}, \dots, a_t, \phi, \dots, \phi), \tau_t + 1)$. The occurrence

of this event is governed only by the delay transition, hence the probability of this event is $\mathbb{P}_\tau(\tau_t + 1 | \tau_t)$.

- *Case 2:* $\tau_{t+1} = 0$. The latest available system state is the most recent system state s_{t+1} . Thus x_{t+1} is $(s_{t+1}, (\phi, \dots, \phi), 0)$. The occurrence of this event is governed by the delay transition with probability $\mathbb{P}_\tau(0 | \tau_t)$ and the system transition from $s_{t-\tau_t}$ to s_{t+1} by executing $\tau_t + 1$ actions $a_{t-\tau_t}, \dots, a_t$, with probability $\mathbb{P}(s_{t+1} | s_{t-\tau_t}, a_{t-\tau_t}, \dots, a_t)$.
- *Case 3:* $0 < \tau_{t+1} \leq \tau_t$. The latest available system state is delayed by τ_{t+1} . Thus x_{t+1} is $(s_{t+1-\tau_{t+1}}, (a_{t+1-\tau_{t+1}}, \dots, a_t, \phi, \dots, \phi), \tau_{t+1})$. Similar to *Case 2*, the occurrence of this event is governed by the delay transition with probability $\mathbb{P}_\tau(\tau_{t+1} | \tau_t)$ and the system transition with probability $\mathbb{P}(s_{t+1-\tau_{t+1}} | s_{t-\tau_t}, a_{t-\tau_t}, \dots, a_{t-\tau_{t+1}})$.

Consequently, we define the transition probability function for the DC-MDP $\mathbb{P}_d : X_d \times \text{Act} \times X_d \rightarrow [0, 1]$ as,

$$\mathbb{P}_d(x_{t+1} | x_t, a_t) = \begin{cases} \mathbb{P}_\tau(\tau_{t+1} | \tau_t), & \text{if } \tau_{t+1} = \tau_t + 1 \\ & x_{t+1} = (s_{t-\tau_t}, (a_{t-\tau_t}, \dots, a_t, \phi, \dots, \phi), \tau_t + 1) \\ \mathbb{P}_\tau(\tau_{t+1} | \tau_t) \underbrace{\sum_{s_{t-\tau_{t+1}} \in S} y_{t-\tau_t} \cdots \sum_{s_t \in S} y_{t-1} y_t}_{\tau_t + 1 \text{ terms}}, & \text{if } \tau_{t+1} = 0, x_{t+1} = (s_{t+1}, (\phi, \dots, \phi), 0) \\ \mathbb{P}_\tau(\tau_{t+1} | \tau_t) \underbrace{\sum_{s_{t-\tau_{t+1}} \in S} y_{t-\tau_t} \cdots \sum_{s_{t-\tau_{t+1}} \in S} y_{t-\tau_{t+1}-1} y_{t-\tau_{t+1}}}_{\tau_t - \tau_{t+1} + 1 \text{ terms}}, & \text{if } 0 < \tau_{t+1} \leq \tau_t \\ & x_{t+1} = (s_{t+1-\tau_{t+1}}, (a_{t+1-\tau_{t+1}}, \dots, a_t, \phi, \dots, \phi), \tau_{t+1}) \\ 0 & \text{otherwise,} \end{cases} \quad (3)$$

where $y_{t-\tau_t} = \mathbb{P}(s_{t-\tau_{t+1}} | s_{t-\tau_t}, a_{t-\tau_t})$ is the one-step transition probability from the system state $s_{t-\tau_t}$ to $s_{t-\tau_{t+1}}$ while executing the action $a_{t-\tau_t}$. We note that the system transition probabilities in *Case 2* and *Case 3* can be factorized into the $\tau_t + 1$ and $\tau_t - \tau_{t+1} + 1$ terms in Eq. 3 respectively. Now, we prove that \mathbb{P}_d is a valid conditional probability distribution with support over the state space X_d .

First we note that since the conditional distributions $\mathbb{P}_\tau, y_t \geq 0, \mathbb{P}_d \geq 0$. Next, we show that $\sum_{x_{t+1} \in X_d} \mathbb{P}_d(x_{t+1} | x_t, a_t) = 1$. Substituting the transition probabilities from *Cases 2,3* in place of the factorized terms in Eq. 3,

$$\begin{aligned} \sum_{x_{t+1} \in X_d} \mathbb{P}_d(x_{t+1} | x_t, a_t) &= \mathbb{P}_\tau(\tau_t + 1 | \tau_t) + \\ &\mathbb{P}_\tau(0 | \tau_t) \sum_{s_{t+1}} \mathbb{P}(s_{t+1} | s_{t-\tau_t}, a_{t-\tau_t}, \dots, a_t) + \\ &\sum_{\tau'=1}^{\tau_t} \mathbb{P}_\tau(\tau' | \tau_t) \sum_{s_{t-\tau'}} \mathbb{P}(s_{t-\tau'} | s_{t-\tau_t}, a_{t-\tau_t}, \dots, a_{t-\tau'-1}). \end{aligned} \quad (4)$$

The inner summations in the second and third terms

of the right-hand side of Eq. 4 equate to 1. Hence, $\sum_{x_{t+1} \in X_d} \mathbb{P}_d(x_{t+1} | x_t, a_t) = \sum_{\tau' \in \Omega} \mathbb{P}_\tau(\tau' | \tau) = 1$.

Thus, the DC-MDP \mathcal{M}_d is the tuple $\langle X_d, \text{Init}_d, \text{Act}, \mathbb{A}, \mathbb{P}_d \rangle$. Additionally, we show how to construct the DC-MDP when only τ_{\max} is known, and \mathbb{P}_τ is not. Since the delay is upper bounded by τ_{\max} , then at any time step t , the action corresponding to the observation $s_{t-\tau_{\max}}$ is always available. Therefore, we take $s_{t-\tau_{\max}}$ as the most recently observed system state and consider the delay to be a constant and equal to τ_{\max} . In this case, our DC-MDP is equivalent to the Constant Delay MDP in [14]. Consequently, the initial delay is set to τ_{\max} and the action buffer is set to $\{(a_s, a_s, \dots, a_s)\}$, where a_s is the action that does not affect the agent's state. In our hardware setup, a_s is the ego-velocity of 0 m/s.

B. Shield Design for Safe Networked Control

In this section, we show how to construct a shield for any MDP $\mathcal{M} = \langle S, \text{Init}, \text{Act}, \mathbb{A}, \mathbb{P} \rangle$, a specification $\varphi = \square \neg S_{\text{unsafe}}$ and a policy π . The shield should ensure that when π is executed in the presence of the shield, the initial state distribution should satisfy φ with at least the desired safety probability δ . First, we formally define the shield.

Definition 1: The ϵ -shield, $C_\epsilon : S \rightarrow 2^{\text{Act}}$, for any state $s \in S$, and $\epsilon \in [0, 1]$ is

$$C_\epsilon(s) = \begin{cases} \{a \mid Q_{\mathcal{M}, \varphi}^{\max}(s, a) \geq \epsilon\} & \text{if } V_{\mathcal{M}, \varphi}^{\max}(s) \geq \epsilon, \\ \{\text{argmax}_a Q_{\mathcal{M}, \varphi}^{\max}(s, a)\} & \text{if } V_{\mathcal{M}, \varphi}^{\max}(s) < \epsilon. \end{cases} \quad (5)$$

During run-time, the action executed is different from $\pi(s)$ only if $\pi(s) \notin C_\epsilon(s)$; in which case an action from $C_\epsilon(s)$ is chosen. Hence, the ϵ -shield is *minimally intrusive*. Now, we show there exists ϵ such that the run-time monitoring of π by the ϵ -shield C_ϵ provides a safety probability greater than δ for the initial states.

Definition 2: The *modified policy*, $\pi_\epsilon : S \rightarrow \text{Act}$, for any state $s \in S$, policy π , and ϵ -shield C_ϵ is

$$\pi_\epsilon(s) = \begin{cases} \pi(s) & \text{if } \pi(s) \in C_\epsilon(s), \\ \text{pick from } C_\epsilon(s) & \text{if } \pi(s) \notin C_\epsilon(s). \end{cases} \quad (6)$$

Observe that the *modified policy* π_ϵ is a result of the run-time monitoring of π by the ϵ -shield C_ϵ . In other words, π_ϵ is the policy that is executed during networked control.

Proposition 1: The safety probability for a state $s \in S$ while executing π_ϵ , $V_{\mathcal{M}, \varphi}^{\pi_\epsilon}(s)$, is lower bounded by $V_{\mathcal{M}_\epsilon, \varphi}^{\min}(s)$ where the MDP $\mathcal{M}_\epsilon = \langle S, \text{Init}, \text{Act}, C_\epsilon, \mathbb{P} \rangle$. The lower bound $V_{\mathcal{M}_\epsilon, \varphi}^{\min}(s)$ is a *non-decreasing* function of ϵ .

Proof: First, we note that executing π_ϵ for \mathcal{M} is equivalent to executing π for $\mathcal{M}_\epsilon = \langle S, \text{Init}, \text{Act}, C_\epsilon, \mathbb{P} \rangle$, where the allowed action set for each state s is given by $C_\epsilon(s)$. Hence, the minimum safety probability for \mathcal{M}_ϵ denoted by $V_{\mathcal{M}_\epsilon, \varphi}^{\min}(s)$ is the lower bound for $V_{\mathcal{M}, \varphi}^{\pi_\epsilon}(s)$.

Now, we show by contradiction that for $\epsilon, \bar{\epsilon} \in [0, 1]$ and $\epsilon < \bar{\epsilon}$, $V_{\mathcal{M}_\epsilon, \varphi}^{\min}(s) \leq V_{\mathcal{M}_{\bar{\epsilon}}, \varphi}^{\min}(s)$ for any state $s \in S$. Assume for the two MDPs, \mathcal{M}_ϵ and $\mathcal{M}_{\bar{\epsilon}}$, $V_{\mathcal{M}_\epsilon, \varphi}^{\min}(s) > V_{\mathcal{M}_{\bar{\epsilon}}, \varphi}^{\min}(s)$ for some state $s \in S$. This implies that the policy that corresponds to $V_{\mathcal{M}_{\bar{\epsilon}}, \varphi}^{\min}(s)$ does not exist for \mathcal{M}_ϵ , and hence $C_\epsilon(s') \subset C_{\bar{\epsilon}}(s')$ for some $s' \in S$. But, from the definition of ϵ -shield, if $\epsilon < \bar{\epsilon}$, then $C_\epsilon(s) \supseteq C_{\bar{\epsilon}}(s) \quad \forall s \in S$, which

is a contradiction. Thus, the lower bound on $V_{\mathcal{M}, \varphi}^{\pi_\epsilon}(s)$, is a *non-decreasing* function of ϵ . ■

Remark 1: For the MDP $\mathcal{M} = \langle S, \text{Init}, \text{Act}, \mathbb{A}, \mathbb{P} \rangle$ and the safety property φ , note that the safety probability for any $s \in S$ is upper-bounded by $V_{\mathcal{M}, \varphi}^{\max}(s)$. So, for the initial state distribution, the upper bound on the safety probability is $\mathbb{E}_{s \sim \text{Init}} [V_{\mathcal{M}, \varphi}^{\max}(s)]$. Hence, any choice of the desired safety probability δ should satisfy $\delta \leq \mathbb{E}_{s \sim \text{Init}} [V_{\mathcal{M}, \varphi}^{\max}(s)]$.

Algorithm 1 Shield Design

Input: MDP $\mathcal{M} = \langle S, \text{Init}, \text{Act}, \mathbb{A}, \mathbb{P} \rangle$, policy π , safety specification $\varphi = \square \neg S_{\text{unsafe}}$, desired safety probability δ

Output: ϵ -shield, C_ϵ^* .

- 1: Initialize ϵ -shield, $C_\epsilon^*(s) = \mathbb{A}(s) \quad \forall s \in S$.
 - 2: Compute $Q_{\mathcal{M}, \varphi}^{\max}(s, a)$ for all state-action pairs in \mathcal{M} .
 - 3: **for** $\epsilon \leftarrow [0, \eta, 2\eta, \dots, 1]$ **do**
 - 4: Determine $C_\epsilon(s)$ for each state $s \in S$ as in Eq. 5
 - 5: Determine the *modified policy* π_ϵ as in Eq. 6.
 - 6: Compute $V_{\mathcal{M}, \varphi}^{\pi_\epsilon}(s)$ for all states in S as in Sec. III.
 - 7: **if** $\mathbb{E}_{s \sim \text{Init}} [V_{\mathcal{M}, \varphi}^{\pi_\epsilon}(s)] \geq \delta$ **then** $C_\epsilon^* = C_\epsilon$
 - 8: **break**
 - 9: **end if**
 - 10: **end for**
 - 11: **return** C_ϵ^* .
-

The Algorithm 1 takes as input the MDP \mathcal{M} , policy π , specification φ , and desired safety probability δ , and outputs the synthesized ϵ -shield C_ϵ^* . In line 2, we compute the maximum safety probability for all state-action pairs in \mathcal{M} , as explained in Sec. III, Eq. 2. Then, we gradually (based on the granularity η) vary the parameter ϵ from 0 to 1 until the safety probability for the initial state distribution, while executing the *modified policy* π_ϵ , is greater than or equal to the desired safety probability δ (lines 3-10).

Theorem 1: (Termination with guaranteed safety). For a given MDP \mathcal{M} and a policy π , Algorithm 1 always terminates with an ϵ -shield, C_ϵ^* as in Eq. 5, such that the *modified policy* π_ϵ , a combination of π and C_ϵ^* (Eq. 6), satisfies the safety property $\varphi = \square \neg S_{\text{unsafe}}$ for the initial state distribution with a probability greater than or equal to the desired safety probability δ , where $\delta \leq \mathbb{E}_{s \sim \text{Init}} [V_{\mathcal{M}, \varphi}^{\max}(s)]$.

Proof: We have shown in Proposition 1 that $V_{\mathcal{M}_\epsilon, \varphi}^{\min}(s)$ is a *non-decreasing* function of $\epsilon \quad \forall s \in S$. Additionally, note that for $\epsilon = 0$, $C_\epsilon(s) = \mathbb{A}(s)$, and therefore $V_{\mathcal{M}_\epsilon, \varphi}^{\min}(s) = V_{\mathcal{M}, \varphi}^{\min}(s)$. Moreover, for $\epsilon = 1$, note that $C_\epsilon(s) = \{\text{argmax}_a Q_{\mathcal{M}, \varphi}^{\max}(s, a)\}$ from Eq. 5. This implies π_ϵ is the same as the optimally safe policy, $\pi_{\mathcal{M}, \varphi}^{\text{safe}}$, from Sec. III. Consequently, we have $V_{\mathcal{M}_\epsilon, \varphi}^{\min}(s) = V_{\mathcal{M}, \varphi}^{\max}(s)$. To summarize, $V_{\mathcal{M}_\epsilon, \varphi}^{\min}(s)$ is a non-decreasing function of ϵ that lies between $V_{\mathcal{M}, \varphi}^{\min}(s)$ and $V_{\mathcal{M}, \varphi}^{\max}(s)$.

Since expectation is a linear operation, $\mathbb{E}_{s \sim \text{Init}} [V_{\mathcal{M}_\epsilon, \varphi}^{\min}(s)]$ is also a non-decreasing function of ϵ that lies between $\mathbb{E}_{s \sim \text{Init}} [V_{\mathcal{M}, \varphi}^{\min}(s)]$ and $\mathbb{E}_{s \sim \text{Init}} [V_{\mathcal{M}, \varphi}^{\max}(s)]$. Therefore, for any desired safety probability $\delta \leq \mathbb{E}_{s \sim \text{Init}} [V_{\mathcal{M}, \varphi}^{\max}(s)]$ (from Remark 1), there

exists an $\epsilon \in [0, 1]$ such that $\mathbb{E}_{s \sim \text{Init}} [V_{\mathcal{M}, \epsilon, \varphi}^{\min}(s)] \geq \delta$. Finally, since $\mathbb{E}_{s \sim \text{Init}} [V_{\mathcal{M}, \varphi}^{\pi_\epsilon}(s)]$ is lower bounded by $\mathbb{E}_{s \sim \text{Init}} [V_{\mathcal{M}, \varphi}^{\min}(s)]$ (Proposition 1), we conclude that the Algorithm 1 always terminates with the ϵ -shield, C_ϵ^* , that guarantees the desired safety probability δ . ■

The choice to pick any action from $C_\epsilon(s)$ when $\pi(s) \notin C_\epsilon(s)$ in Eq. 6 does not affect the ϵ -shield construction as outlined in Algorithm. 1. One could select actions from $C_\epsilon(s)$ prioritizing either task-efficiency or safety ($\arg\max_a Q_{\mathcal{M}, \varphi}^{\max}(s, a)$), and Algorithm 1 still holds true. Additionally, our shield construction approach is very generic and applicable to any MDP, safety specification and policy. Therefore, for safe networked control, we first construct the DC-MDP (as described in Sec. V-A), and given the safety specification $\varphi = \square \neg S_{\text{unsafe}}$ and the cloud controller π_{cloud} , we use Algorithm 1 to construct the ϵ -shield, C_ϵ^* , that ensures safety probability greater than δ for the initial states.

Remark 2: Algorithm 1 can be modified to yield an ϵ -shield even when π is not known, in cases like human-teleoperation. Since the *modified policy* cannot be computed without π , we instead check for $\mathbb{E}_{s \sim \text{Init}} [V_{\mathcal{M}, \varphi}^{\min}(s)] \geq \delta$ in line 7 of the Algorithm 1. This guarantees safety probability of at least δ for any *modified policy* π_ϵ .

VI. EXPERIMENTS

Now, we show empirically that the shield ensures safety in the presence of communication delays. We also contrast the behavior of the agent with shields constructed using two different DC-MDPs: “constant delay” when maximum delay τ_{max} is known, and “random delay” when in addition the delay transition probability \mathbb{P}_τ is modeled. Moreover, we observe that the trade-off between safety and task efficiency is naturally handled by the shield. It forces the agent to act conservatively during higher delays and enables aggressive behavior during lower delays. We test on three environments,

- A 2D 8×8 gridworld simulation setup where the controlled robot, initialized at (0,0), is tasked with reaching the goal at (7,7) while avoiding collision with a dynamic obstacle. Each episode runs for 50 timesteps. An episode is considered a *win* if the robot reaches the goal without colliding, a *loss* if there is a collision, or a *draw* otherwise. The cloud controller is learned using tabular Q-learning.
- A car-following simulation setup where the ego robot has to follow the leader car while maintaining a minimum safety distance of 5m. The system state consists of relative distance and relative velocity. The leader car can accelerate at anywhere between -0.2m/s^2 and 0.2m/s^2 , and the ego robot can accelerate between -0.5m/s^2 and 0.5m/s^2 . Each episode runs for 100s. The cloud controller is a pre-trained RL agent that maximizes distance traveled and minimizes collisions with the leader. To obtain a finite state space for the MDP, we discretize to the closest and smallest discrete points like (5m, 6m, ...) for relative distance and (-5m/s , -4.5m/s ...) for relative velocity.
- The hardware setup (see Fig. 2) with two F1/10th vehicles [16]. The ego robot is equipped with a Hokuyo Laser

rangefinder that generates a point cloud of 1080 values which is transmitted over WiFi using ROS to a remote Nvidia desktop GPU (the cloud). Here the state is estimated and a time-optimal control command is sent back over WiFi to the robot. The robot’s objective is to follow the leader as quickly as possible while maintaining a safe distance of at least 0.2m between the cars.

For the car-following and the hardware setup, the safety specification is $\square \neg S_{\text{unsafe}}$, where S_{unsafe} consists of states where the distance between the cars is less than 5m and 0.2m respectively. For the gridworld, it is $\neg S_{\text{unsafe}} \cup \text{success}$, where S_{unsafe} is the set of states which have the robot and obstacle in the same position: a collision and success is when the robot is at the goal and the obstacle is not.

How does the performance of our safe networked control approach vary with communication delay? The safety of the teleoperated robot reduces when the communication delay increases. We observe this in Figs. 3a and 3d for the two simulation setups, for the constant delay case. The set of states for which maximum safety probability $V_{\mathcal{M}, \varphi}^{\max}(s)$ (Sec. III) is greater than a δ value shrinks with increasing delay. It shows that when the delay is large it is safer for the robot to stay farther away from the dynamic obstacle (gridworld) and for the ego robot to maintain a larger relative distance and velocity between itself and the leader car (car-following).

The shields ensure the desired safety probability δ for different delays. However, for the same safety probability, the task performance degrades with increasing delay due to increasing uncertainty in the system state. We show this quantitatively for the two simulation setups with constant delay. In the gridworld, with larger delays, the shield increasingly restricts the robot from moving aggressively towards the goal to avoid collisions. As such, it effectively sacrifices a win for a tie. Similarly, in the car-following scenario, the distance maintained from the leader robot increases (Fig. 3c). We observe a similar trend in our hardware setup that runs on a wireless network with stochastic delays (Fig. 4a). During the initial 10s, when the delay is less than 100 ms, the average distance maintained is less than 1.25 m. Then, when the delay is about 200 ms, the ego-robot starts to maintain a larger distance of around 1.5 m.

How does δ affect the safety-efficiency trade-off? Our key insight is that we can vary δ to trade off safety for task efficiency. We observe this in the constant delay case, where increasing δ leads to increasingly conservative behavior with more restrictions from the shield. In the gridworld, Fig. 3f shows fewer wins and more ties, an indicator of reduced task efficiency. Additionally, the number of losses decreases as safety is prioritized. Similarly, for car-following, the average distance maintained from the leader car increases (Fig. 3c). On the other hand, $\delta = 0$ is the un-shielded approach, which leads to a violation of the safety specification.

How does incorporating the delay transition probability function \mathbb{P}_τ affect safety and efficiency? We now illustrate that by incorporating \mathbb{P}_τ , our safe networked control approach performs more efficiently since the DC-MDP model is more accurate. Whereas, when only τ_{max} is known, the

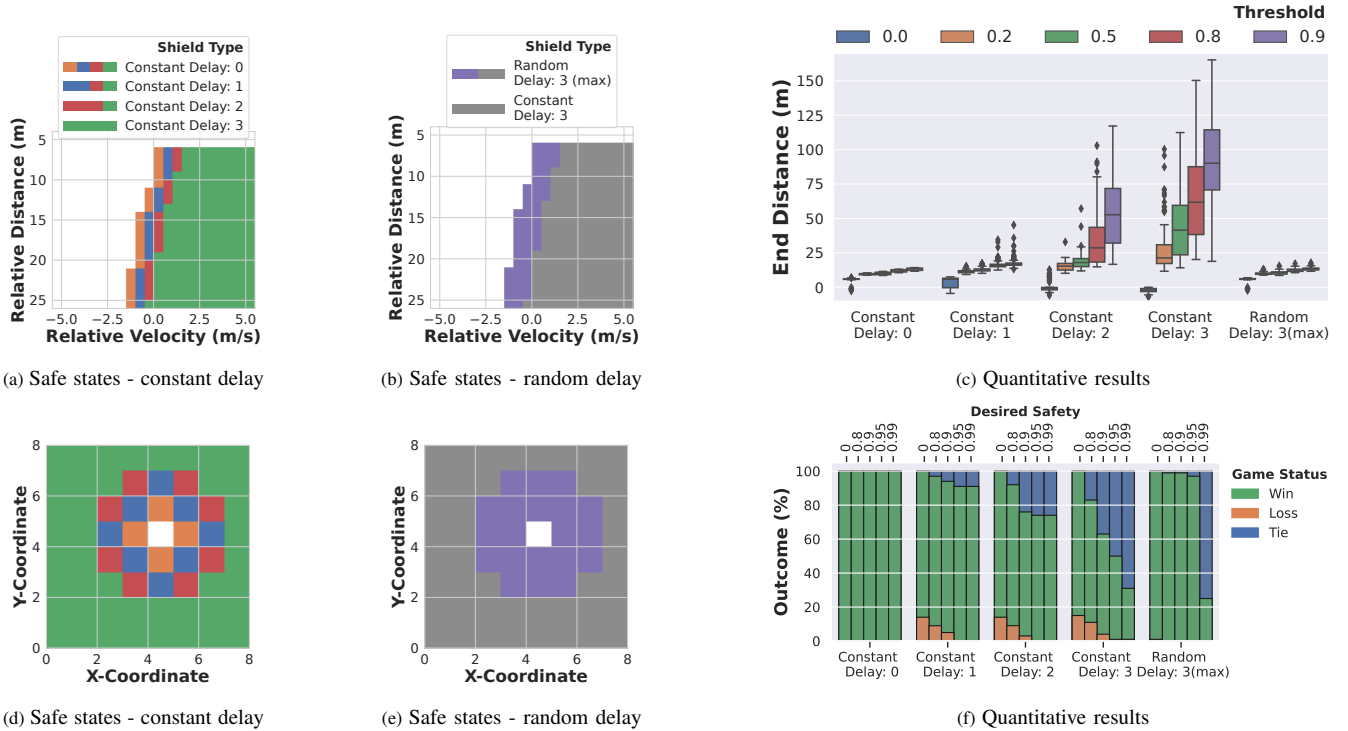


Fig. 3: **Shielding leads to safe networked control in simulations.** Top row - Car following simulation results; Bottom row - Gridworld simulation results. Figs. 3a and 3d show the set of safe initial states with maximum safety probability greater than 0.95 for the *Delayed Communication* MDP for the constant delay case. The set of safe states expands as the maximum delay (τ_{\max}) decreases. This is depicted by the legend that has multiple colors attributed to lower latencies. Figs. 3b and 3e compares the set of safe initial states with maximum safety probability greater than 0.95 for the random and constant delay cases with $\tau_{\max} = 3$ in both the cases. The set of safe states is larger in the case of random delay as the shield exploits the knowledge of the delay transitions to allow the agent to act more aggressively. The white color represents initial states that have maximum safety probability less than 0.95. For the gridworld setup, the obstacle is located at (4,4). Figs. 3c and 3f show that as latency increases, the system tends to be conservative, leading to increased distances in the car-following scenario, and an increased number of ties in the gridworld case.

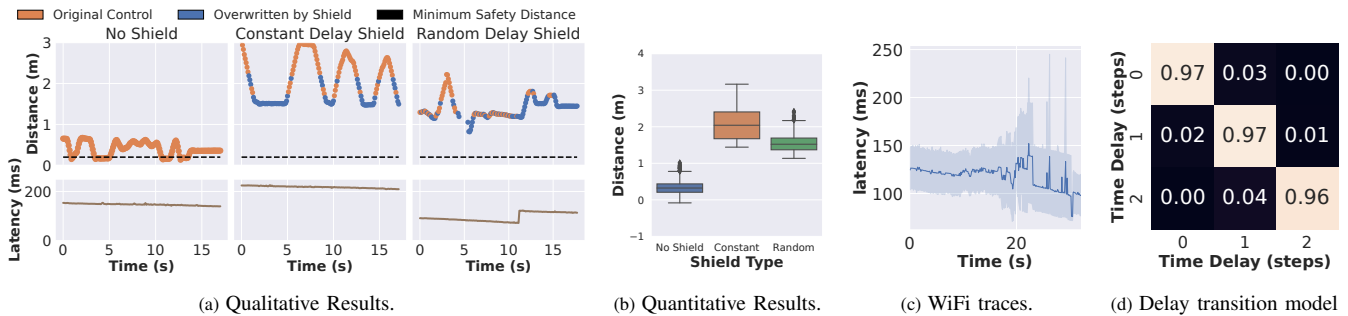


Fig. 4: **Real World Demonstration Results.** Fig. 4a shows recorded trajectories from our hardware setup. Without our safe networked control approach, the system fails to satisfy the safety specification “always remain at least 0.2 meters away”. However, our approach can satisfy the safety specification for constant and random delays. Also, as seen in Fig. 4b, the shield for the random delay case exploits the knowledge of delay transitions in Wi-Fi rather than assuming only the maximum latency, which allows the ego robot to follow the leader car at a closer distance. We set $\epsilon = 0.95$ to construct the ϵ -shield. In Fig. 4c and Fig. 4d, we show how the delay transition probability function, \mathbb{P}_τ , is estimated using multiple runs of the Wi-Fi latency time-series data. Here, \mathbb{P}_τ is a conditional probability distribution with 3 possible delays (0, 1, 2), where each delay is a bin of size 100 ms.

model is less accurate as it assumes the observation from τ_{\max} steps before to be the latest available system state even if the delay is small and more recent system states are available. We compare the DC-MDP for constant delay of $\tau_{\max} = 3$ against the DC-MDP for random delay with an assumed \mathbb{P}_τ . Firstly, Figs. 3b and 3e show that the set of states for which maximum safety probability $V_{\mathcal{M},\varphi}^{\max}(s)$ (Sec. III) is greater than a δ value is larger when \mathbb{P}_τ is incorporated. Secondly, we observe more wins and fewer draws in the gridworld, and lower aggregate distance maintained for the

car following setup as seen in Figs. 3f and 3c respectively. For the hardware setup, \mathbb{P}_τ is obtained experimentally (see Fig. 4d). Similar to the car following setup, the distance maintained between the two robots is less in the case of random delay when compared to constant delay (see Fig. 4b). This difference in safety distance is statistically significant with a Wilcoxon p-value < 0.001 . To summarize, we infer that incorporating \mathbb{P}_τ in our DC-MDP design allows for efficient task performance *without* compromising safety.

Does a minimally intrusive shield always lead to safety?

Fig. 4a shows the state trajectory in the presence and absence of the ϵ -shield, and the instances when the ϵ -shield overwrites the cloud controller of the hardware setup. The ϵ -shield overwrites control commands when close to the leader car (relatively unsafe), and is inactive when further away. For example, in the constant delay case, the shield is inactive when the distance is above $\sim 2.25\text{m}$. However, this does not affect safety.

Limitations: Though our approach accurately captures the system transitions in the presence of random delays, this comes at the cost of exponential increase in size of the DC-MDP. However, through our experiments, we note that even for significant communication delays of 400 or 500 ms, discretized to 4 or 5 time steps, our approach scales well.

VII. CONCLUSION AND FUTURE DIRECTIONS

This paper provides a novel approach to accurately model the networked control system transitions in the presence of stochastic communication delays as an MDP. Consequently, we use the MDP to synthesize shields for safe networked control. We demonstrate our approach on simulation and hardware setups. Our work is timely since we are seeing a surge of teleoperated robots.

We note that there could exist multiple approaches to filter actions that are sub-optimal with respect to safety, other than Eq. 5. Focusing on these other approaches could be an interesting future work. Additionally, exploring state space reduction techniques to handle the exponential growth of state space in DC-MDP is another interesting future work.

REFERENCES

- [1] I. El Rassi and J.-M. El Rassi, "A review of haptic feedback in tele-operated robotic surgery," *Journal of medical engineering & technology*, vol. 44, no. 5, pp. 247–254, 2020.
- [2] O. El Marai, T. Taleb, and J. Song, "Ar-based remote command and control service: Self-driving vehicles use case," *IEEE Network*, 2022.
- [3] J. Wong, A. Tung, A. Kurenkov, A. Mandekar, L. Fei-Fei, S. Savarese, and R. Martín-Martín, "Error-aware imitation learning from teleoperation data for mobile manipulation," in *Conference on Robot Learning*. PMLR, 2022, pp. 1367–1378.
- [4] "Who's driving that food delivery bot? it might be a gen z gamer," <https://www.latimes.com/business/story/2022-03-17/california-autonomous-sidewalk-food-delivery-robots-coco-starship-kiwibot>, 2022, [Online; accessed 03-Feb-2022].
- [5] S. Bansal, M. Chen, S. Herbert, and C. J. Tomlin, "Hamilton-jacobi reachability: A brief overview and recent advances," in *2017 IEEE 56th Annual Conference on Decision and Control (CDC)*. IEEE, 2017, pp. 2242–2253.
- [6] J. F. Fisac, N. F. Luvovoy, V. R. Royo, S. Ghosh, and C. J. Tomlin, "Bridging hamilton-jacobi safety analysis and reinforcement learning," *2019 International Conference on Robotics and Automation (ICRA)*, pp. 8550–8556, 2019.
- [7] R. Cheng, G. Orosz, R. M. Murray, and J. W. Burdick, "End-to-end safe reinforcement learning through barrier functions for safety-critical continuous control tasks," in *AAAI Conference on Artificial Intelligence*, 2019.
- [8] J. Choi, F. Castañeda, C. J. Tomlin, and K. Sreenath, "Reinforcement learning for safety-critical control under model uncertainty, using control lyapunov functions and control barrier functions," in *Robotics: Science and Systems (RSS)*, 2020.
- [9] M. Alshiekh, R. Bloem, R. Ehlers, B. Könighofer, S. Niekum, and U. Topcu, "Safe reinforcement learning via shielding," in *Proceedings of the AAAI Conference on Artificial Intelligence*, vol. 32, no. 1, 2018.
- [10] S. Carr, N. Jansen, S. Junges, and U. Topcu, "Safe reinforcement learning via shielding under partial observability," in *AAAI*, 2023.
- [11] N. Jansen, J. Junges, and A. Serban, "Safe reinforcement learning using probabilistic shields," 2020.
- [12] B. Könighofer, F. Lorber, N. Jansen, and R. Bloem, "Shield synthesis for reinforcement learning," in *Leveraging Applications of Formal Methods, Verification and Validation: Verification Principles: 9th International Symposium on Leveraging Applications of Formal Methods, ISOFA 2020, Rhodes, Greece, October 20–30, 2020, Proceedings, Part 1 9*. Springer, 2020, pp. 290–306.
- [13] S. Adlakha, S. Lall, and A. Goldsmith, "Networked markov decision processes with delays," *IEEE Transactions on Automatic Control*, vol. 57, no. 4, pp. 1013–1018, 2011.
- [14] K. V. Katsikopoulos and S. E. Engelbrecht, "Markov decision processes with delays and asynchronous cost collection," *IEEE transactions on automatic control*, vol. 48, no. 4, pp. 568–574, 2003.
- [15] E. Derman, G. Dalal, and S. Mannor, "Acting in delayed environments with non-stationary markov policies," in *International Conference on Learning Representations*, 2020.
- [16] M. O'Kelly, V. Sukhil, H. Abbas, J. Harkins, C. Kao, Y. V. Pant, R. Mangharam, D. Agarwal, M. Behl, P. Burgio *et al.*, "F1/10: An open-source autonomous cyber-physical platform," *arXiv preprint arXiv:1901.08567*, 2019.
- [17] C. Baier and J.-P. Katoen, *Principles of model checking*. MIT press, 2008.
- [18] B. Kehoe, S. Patil, P. Abbeel, and K. Goldberg, "A survey of research on cloud robotics and automation," *IEEE Trans. Automation Science and Engineering*, vol. 12, no. 2, pp. 398–409, 2015.
- [19] J. Kuffner, "Cloud-enabled robots in: Ieee-ras international conference on humanoid robots," *Piscataway, NJ: IEEE*, 2010.
- [20] A. K. Tanwani, N. Mor, J. D. Kubiatowicz, J. E. Gonzalez, and K. Goldberg, "A fog robotics approach to deep robot learning: Application to object recognition and grasp planning in surface decluttering," *2019 International Conference on Robotics and Automation (ICRA)*, pp. 4559–4566, 2019.
- [21] S. Chinchali, A. Sharma, J. Harrison, A. Elhafi, D. Kang, E. Pergament, E. Cidon, S. Katti, and M. Pavone, "Network offloading policies for cloud robotics: a learning-based approach," *Autonomous Robots*, pp. 1–16, 2021.
- [22] G. Mohanarajah, D. Hunziker, R. D'Andrea, and M. Waibel, "Rapyuta: A cloud robotics platform," *IEEE Transactions on Automation Science and Engineering*, vol. 12, no. 2, pp. 481–493, 2015.
- [23] N. Tian, A. K. Tanwani, K. Goldberg, and S. Sojoudi, "Mitigating network latency in cloud-based teleoperation using motion segmentation and synthesis," in *Robotics Research: The 19th International Symposium ISRR*. Springer, 2022, pp. 906–921.
- [24] T. Lancewicki, A. Rosenberg, and Y. Mansour, "Learning adversarial markov decision processes with delayed feedback," in *Proceedings of the AAAI Conference on Artificial Intelligence*, vol. 36, no. 7, 2022, pp. 7281–7289.
- [25] S. Pranger, B. Könighofer, M. Tappler, M. Deixelberger, N. Jansen, and R. Bloem, "Adaptive shielding under uncertainty," in *2021 American Control Conference (ACC)*, 2021, pp. 3467–3474.
- [26] B. Könighofer, J. Rudolf, A. Palmisano, M. Tappler, and R. Bloem, "Online shielding for reinforcement learning," *Innovations in Systems and Software Engineering*, pp. 1–16, 2022.
- [27] W.-C. Yang, G. Marra, G. Rens, and L. De Raedt, "Safe reinforcement learning via probabilistic logic shields," *arXiv preprint arXiv:2303.03226*, 2023.
- [28] M. Bouton, J. Karlsson, A. Nakhaei, K. Fujimura, M. J. Kochenderfer, and J. Tumova, "Reinforcement learning with probabilistic guarantees for autonomous driving," *arXiv preprint arXiv:1904.07189*, 2019.
- [29] D. Aksaray, Y. Yazıcıoğlu, and A. S. Sarkaya, "Probabilistically guaranteed satisfaction of temporal logic constraints during reinforcement learning," in *2021 IEEE/RSJ International Conference on Intelligent Robots and Systems (IROS)*. IEEE, 2021, pp. 6531–6537.
- [30] A. J. Taylor, A. W. Singletary, Y. Yue, and A. D. Ames, "Learning for safety-critical control with control barrier functions," in *Conference on Learning for Dynamics & Control*, 2019.
- [31] A. Nasrallah, A. S. Thyagaturu, Z. Alharbi, C. Wang, X. Shao, M. Reisslein, and H. ElBakoury, "Ultra-low latency (ull) networks: The ieee tsn and ietf detnet standards and related 5g ull research," *IEEE Communications Surveys & Tutorials*, vol. 21, no. 1, pp. 88–145, 2018.
- [32] C. Liu, T. Arnon, C. Lazarus, C. Strong, C. Barrett, M. J. Kochenderfer *et al.*, "Algorithms for verifying deep neural networks," *Foundations and Trends® in Optimization*, vol. 4, no. 3-4, pp. 244–404, 2021.